ISSN -2319-3166

STUDENT JOURNAL OF PHYSICS

Volume 4 Number 6 Jan.-Mar. 2013

INDIAN ASSOCIATION OF PHYSICS TEACHERS

STUDENT JOURNAL OF PHYSICS

This is a quarterly journal published by Indian Association of Physics Teachers. It publishes research articles contributed by Under Graduate and Post Graduate students of colleges, universities and similar teaching institutions, as principal authors.

Indian Association of Physics Teachers (IAPT)
Central Office :
Indian Institute of Education Campus
128/2 J.P. Naik Road, Kothrud, Pune-411038
E-mail : centraloffice@iapt.org
Phone : 91 20 2545 5504

Registered Office

L 117/302, Naveen Nagar, Kanpur – 208 025

Manuscripts may be submitted in appropriate format to any of the editors.

For more information about subscription, membership, renewals, address changes, etc., enquiries should be addressed to the Managing Editor.

Editorial

Soft Power and Indian Science

It is distressing to note that none of the Indian universities and higher teaching Institutions like IITs and ISERs etc. figure in the list of 200 universities in the latest (2012) QS World University Rankings. Many Asian countries have qualified for the distinction with seven universities of China occupying the positions 44, 48, 89, 125, 168, 170 and 186; and even Malaysia and Saudi Arabia capturing the spots 156 and 197 respectively. Anguish has been expressed over this by many distinguished citizens in various fora, the most conspicuous being the public lament by the President of India in his convocation address at the Utkal University, Bhubaneswar in last April. It becomes all the more intriguing and poignant when one is reminded of the glorious heritage of India, with one of the earliest civilization of the world of about 5000 years old, credited with gigantic contribution to various fields of human knowledge spanning literature, philosophy, science, mathematics, music and religion etc., possessing the unique distinction of unbroken continuity up to the modern age. More strikingly, the vast expansion of our education system after independence with the establishment of more than 600 universities, dozen of IITs, several IISERs, NISER, and more than 100 of national laboratories and research institutes has earned it the reputation of being the largest educational system in the world. Needless to mention that many of our top ranking institutions are in no way less equipped in terms of infrastructure and facilities compared to their counter parts in the western world.

The spectacular achievement of Indian science in the first half of twentieth century before independence, through the works of C.V. Raman, J.C. Bose, M.N. Saha, H.J. Bhabha, S.N. Bose et. al. carried out in a couple of Indian universities with meager facilities worth the name, defies all sense of logic and reason, when contrasted with the current scenario. How does one reconcile the present lack lustre and dismal performance of Indian universities and higher institutions of learning not being able to occupy a single position in the list of top 200 universities in the world? Presently, our country is an impoverished soft power in science, although it can be considered a hard power as the above data suggests. The present scientific culture is not empowering it to take a leading role in international science. What is culture? The values, ethos, faith, thought and understanding collectively held by a nation, people or community and their outward manifestation in the form of customs, ways of working, taste, sensitivity and sensibility can perhaps qualify to be a concise definition. At the core, there is an underlying passion guiding the thought and action of every member of the community towards a goal without his apparent consciousness. Thus it is an invisible force directly and imperceptibly operating on the minds of the individual in the collective body and guiding the achievement, success and fulfillment in life.

The buzzword is collectivity. One may remember that, human civilization was born and flourished when pre-historic man came together and participated in living, hunting, food collecting, fighting against wild animals and vagaries of nature forming a society. Does India have a viable scientific/academic community similar to those of western countries? Before independence we had a small scientific community scattered in few universities and colleges. However it was regarded as a part of British community which was most flourishing and dominant at the world level. Britain was then the centre of gravity of international science and the seat of biggest global power in the history. Needless to mention the Nobel Prize of C. V. Raman in physics and that of Ravindranath Tagore in literature are considerably supported by the common bond of fraternity of this larger community. The small Indian community was undoubtedly imbued with its soft power. Unfortunately in the post independence era, we have not been able to create a viable self-supporting community of our own with the required passion, values, ethos and vision to inspire us, to play a dominant role in international science although the nation has invested substantially in developing its hard power. Feudalism and cronyism, the legacy of the past thousand years of history is weighing heavily on our consciousness and polluting the educational and scientific sphere of the country rendering them lack lusture. The specific example of the physics journal PRAMANA can be cited here. It was started in mid 1960s with great hope to act as the vehicle to carry Indian innovative ideas to the international arena. It has not succeeded and the country has to depend upon the western journals for the same. In 1978, when the author was visiting Niels Bohr Institute, Copenhagen, he had the pleasant experience of meeting a senior physicist from Japan, who gave the following suggestions to improve Indian science. "Firstly the manuscript submitted to journals for publication should be neatly typed to avoid rejection, which was relevant then. Secondly India should have its own journal with international circulation for publication of its new ideas, which would be an uphill task for acceptance in western journals." When I asked what they do in Japan, he replied; "(1) We first publish our new ideas in Japanese journals. (2) Then we submit the same to international conferences, which we attend with large number of colleagues to defend it. (3) Finally we submit to international journals.

H. Yukawa was awarded Nobel Prize in 1949 for meson theory of nuclear force which he published in the form of eight papers in Japanese journals. This practice has been continuing in Japan with rich dividends. It is in fact a common feature with other advanced nations. Before the advent of European Union, all its constituent countries small and big, were nurturing their own journals for such contingency.

Soft power cannot be enhanced by investment of large amount of funds by the country into science, nor by enactment of any law but by enlightened awareness and conscious effort of nurturing the culture cited above by the science fraternity, more so by its leaders.

L. Satpathy

TURNING POINTS

Re-Creating the Big Bang

Rajiv V. Gavai
Department of Theoretical Physics, Tata Institute of Fundamental Research, Homi Bhabha Road, Mumbai 400005, India

Abstract. A few microseconds after the Big Bang, our Universe may have been dominated by a hitherto undiscovered phase, called Quark-Gluon Plasma (QGP). The theory of strong interactions, Quantum Chromo Dynamics (QCD), **predicts** a transition of the strongly interacting matter to Quark-Gluon Plasma at high temperatures and/or densities. Heavy ion collision experiments at very high energies at Brookhaven National Laboratory, New York and CERN, Geneva have the potential for producing the right conditions for such a transition to occur. This introductory review of the subject is aimed at explaining what quark-gluon plasma is, why it is important and how it can be created and studied in the laboratory. Unlike other interactions in nature, the QCD coupling, a measure of its strength of interaction, can be very strong, thereby necessitating new theoretical tools. QCD on a space-time lattice is the most reliable such tool available to us. Lattice QCD on Supercomputers has enabled us to predict both the transition to QGP phase and the properties of the QGP phase. The same techniques also predict a QCD critical point which experiments have begun actively to search for. Indian efforts in both theoretical and experimental directions are very strong in these areas.

Communicated by: D.P. Roy

1. INTRODUCTION: WHAT IS THE BIG BANG ?

All ancient civilizations, including our own Indian civilization, have wondered about the origins of the Universe we find ourselves in. Questions like what we, and the world around us, are made of and how our Universe began, i.e., if it did have a beginning, have consumed all of us. The common answers we heard as children were that of *"Panch Mahabhoota"* and concepts like *"Pralaya"* etc. Others, e.g., the Greek and other western civilizations also had similar ideas. It was, however, after the great observational research work of the likes of Galileo and Kepler, and the laying of theoretical foundations by people like Newton, that modern science slowly began dominating our methodology to answer such questions. Amazingly, humongous progress has been made in coming closer to the answers of such questions. Indeed, as Einstein once remarked, "what is really incomprehensible is that our Universe is so comprehensible to us at all." . Today we all are aware of molecules and atoms as the basic building blocks of the matter around us, including we ourselves. Similarly, we have learnt about our Solar system and the fact that our Earth is a planet which revolves round the Sun to give us the seasons we enjoy. Observations played a critical role in building up these concepts. Galileo used the telescope to advance our knowledge of our Solar system. Microscopes revealed to us the marvels of the otherwise invisible world of smaller objects. Essentially the same idea of using telescopes and microscopes, but bigger and more powerful ones, have lead us further beyond the above mentioned picture we learn in the school. Thus, we now know that our Sun is just one star out of the many crores of stars in our galaxy, called Milky Way (*Aakashganga* in Marathi).

Our Universe has crores of such galaxies. One way to imagine all these mind-bogglingly huge numbers, and the size of the Universe they imply, is to use the fact that light travels very fast, about 300, 000 kilometers in one second. Let us call this distance one light-second. The diameter of our Earth is about 0.0425 light-seconds and our Sun is 499 light-seconds, i.e. 8.317 light-minutes away from us. So we say light from our Sun takes about 8 minutes to reach us. The light from the closest star takes about 4.22 years to reach us while it takes about 100,000 years to cross our disc shaped Milky Way galaxy. The size of our Universe in these same units is 156 abja (billion) light years ! Surprisingly, we still can claim to understand in a simple way how the Universe began and evolved. To be sure, many details are still missing and will need to be plugged in after further research. I will narrate a part of the story of our Universe below which amazingly can perhaps be re-created in the laboratory.

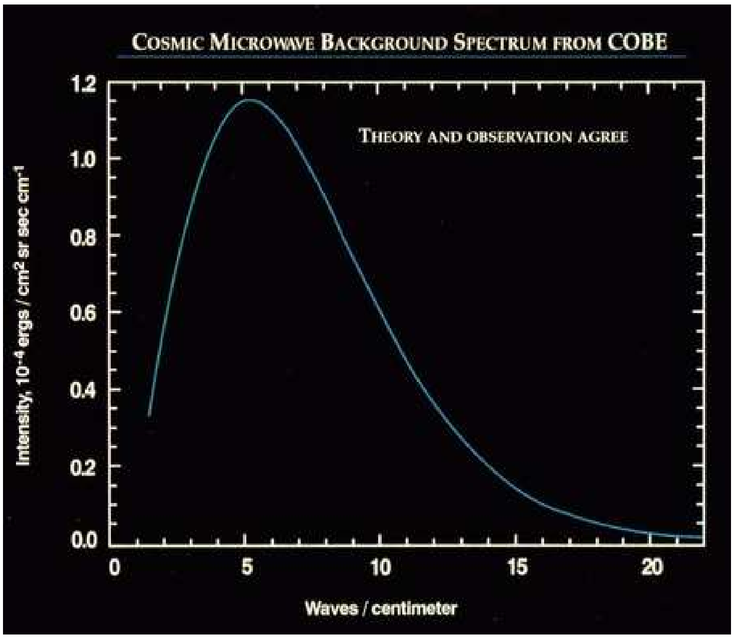

Figure 1. COBE measurement [2] of the cosmic microwave background radiation. Its peak location measures the temperature of our Universe 380,000 years ago.

Edwin Hubbles observation of stellar objects lead him to propounding a law for them: Distant galaxies move away from us at a rate proportional to their distance (as measured by their red-shift). This in turn led to a picture of our Universe as having been denser in the past than now. The Big Bang theory of Universe accounts for this law by the assertion that our Universe was born in a hot, giant explosion and subsequently cooled by expansion[1]. The strongest evidence to date for this theory has come from the increasingly precise measurements of the cosmic microwave background radiation (CMBR), shown in the Figure 1. In spite of displaying the error bars on the observed data a couple of hundred times more than actually are, one sees such a perfect agreement of the theoretical black body curve with the data such that the latter are totally invisible. In fact, this is the most perfect observed black body radiation spectrum ever. It can be used to determine the temperature of our entire Universe today. Its perfection enables us to'measure' the rather low temperature of our Universe to an incredible precision.

The temperature thus measured is of that epoch of the Universe at which electromagnetic radiation decoupled from matter: $T \approx 3000 \deg K$, red-shifted due to the expansion of our Universe to $T = 2.726 \deg K$. Using the fluctuations in this background temperature, astronomers from WMAP satellite experiment have even constructed the earliest picture of our Universe at about 380,000 years of its age.

A natural consequence of the expansion is that the Universe was much hotter at earlier times. If we understand well the physics of those early times, or at very high temperatures, then we will be able to glance into still earlier times in the history of the Universe. Thus, e.g., our extensive knowledge of the many nuclear reactions has enabled us to estimate the compositions of our Universe in terms of the basic elements. Its confirmation by observations has inspired confidence in our scenario up to about the first three minutes of the age of the Universe. As we approach the big bang itself, the next new landmark of physics is at about 10-20 s, corresponding to the formation of protons and neutrons from a hitherto unobserved state of matter called Quark-Gluon Plasma[3]. At a few microseconds after the Big Bang, our Universe may have been dominated by quark-gluon plasma (QGP). Heavy ion collision experiments at very high energies at Brookhaven National Laboratory, New York and now at the Large Hadron Collider in CERN, Geneva have the potential for producing the right conditions for such a phase transition to occur. This introductory review of the subject endeavours to explain what quark-gluon plasma is, why it is important and how it can be created and studied in laboratory.

1.1 *Why Re-Create the Big-Bang ?*

The known interactions a century ago were Electromagnetism & Gravity and the then known elementary particles were electrons and atoms. We all learn about them in schools. Rutherford's classic scattering experiment, and its subsequent sophisticated versions in form of high energy particle accelerators and detectors, yielded various new layers of building blocks. Thus, we now know that the atoms are further made of electrons surrounding nuclei. Their numbers and properties decide the property of the material such as conductors and insulators. The nucleus itself is made from proton, neutrons and pions. In turn, these particles are further made from even tinier quarks and gluons. The best way to imagine them is to think of their sizes. A typical atom is a few Angstroms in size, i.e, about one croreth part of the centimetre we use in daily life. A nucleus is roughly 10000 times smaller than an atom, and a quark is further 1000 times smaller, almost the same size as that of an electron, also called a lepton. Quarks and leptons are today regarded as the elementary particles from which our matter is made. Protons and neutrons make up the nuclei discovered by Rutherford, while they themselves are made up of quarks: Proton(Neutron)consists of two u(d) type of quarks and one d(u) quark while a pion, regarded as the key behind the nuclear force, is made of a u-quark and d-antiquark.

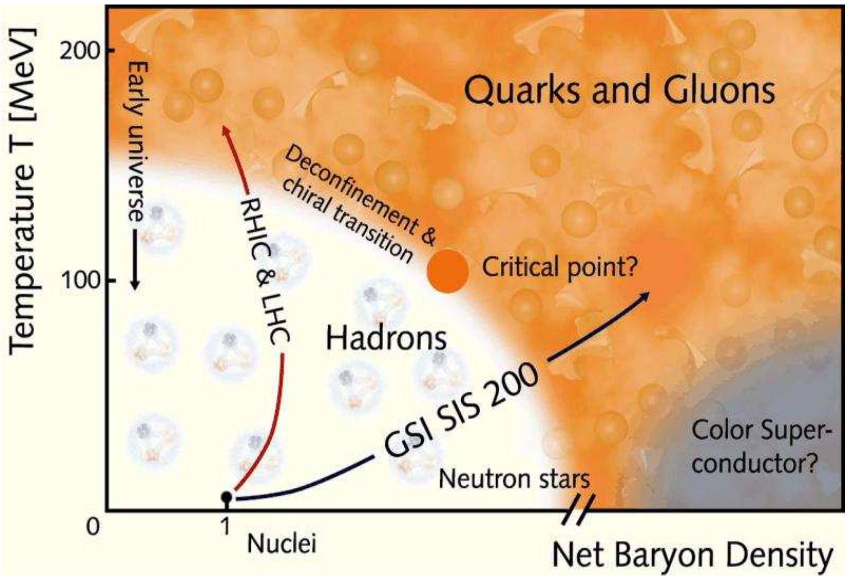

Figure 2. Expected QCD phase diagram. We hope to establish the QCD critical point and other features by better theoretical and experimental efforts in the future.

Over the years, strong and weak nuclear forces got added to the list of forces. A variety of vector bosons act as the carriers of these forces. The strengths of these forces are substantially different. While the electromagnetic interaction is two orders of magnitude smaller than the strong interactions which bind quarks together into protons and neutrons, it is an order of magnitude larger than the weak nuclear force. Massless gluons are the vector particles which carry the strong interaction whereas massive W and Z-bosons (80 times mass of the proton) carry the weak nuclear force. Gravity, the most familiar force is the weakest force being smaller by about 37 orders of magnitude than the electromagnetic force. These become relevant in controlling the history of our Universe close to the instant of the big bang (a billionth of a billionth of a billionth of a billionth of second after the big bang) whereas the weak interaction played the dominant role a few nanoseconds after the Big Bang. So far, we have no good idea of how to study matter at such early times. It is an interesting challenge to come up with an idea to do so. On the other hand, we do have experimental tools to produce matter that may have existed in our Universe a few microseconds after the Big Bang in a laboratory. Furthermore, we also have a theory for the strong nuclear force, as well as a method of computation for it, to derive the properties of matter under such conditions at that time, as we shall discuss below.

2. PHASE DIAGRAM OF STRONG MATTER

2.1 *Some results*

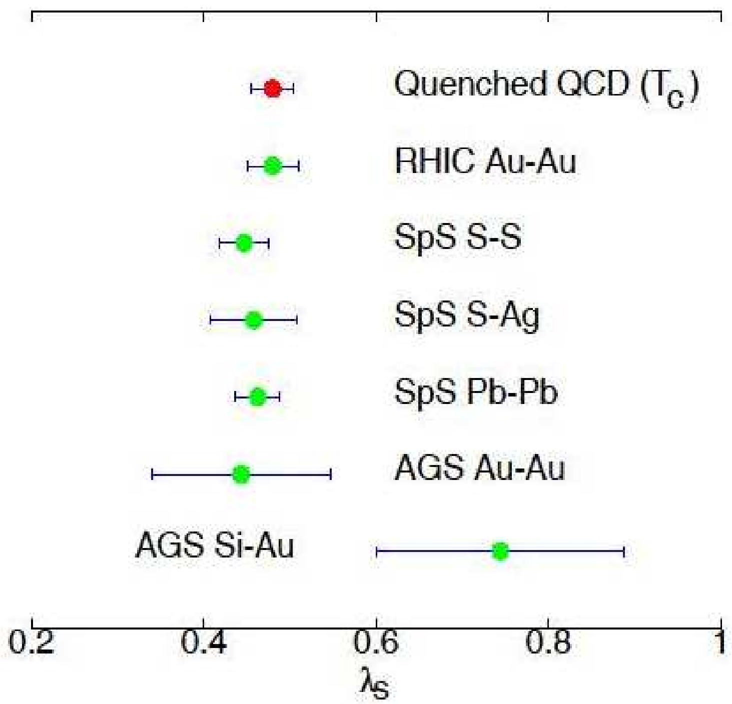

Figure 3. Experimental results for the excess strangeness produced in nucleus-nucleus collisions compared to lattice QCD results[4].

Quantum Chromo Dynamics (QCD) is the (gauge) theory of (strong) interactions of quarks and gluons. The strength of this force as well as its complexity leads to a much richer structure: Quarks are permanently confined to hadrons like proton and neutrons; a dynamical symmetry breaking ensures that the quarks become massive due to interactions although free quarks are rather light etc. These and many more such properties need to be obtained from QCD. While in the early days of strong interactions, one attempted to understand these features based on models, we now have a powerful technique, called lattice field theory, to derive them from the basic theory. Indeed, fifty years after the discovery of proton and neutron was it possible at all to calculate their masses and their structure from this basic underlying theory QCD using lattice field theory techniques. This same lattice technique, as well as certain models, predict new phases of matter at high temperatures and densities shown in the Figure 2. Quark-Gluon Plasma is one such new phase. It is expected to be produced in Relativistic Heavy Ion Collisions as we shall see in the next section. Its experimental confirmation will test the predictions of the theory of strong interaction QCD in a new domain. Moreover, since such temperatures are relevant to our Universe at a few microseconds after the big bang, these collisions will permit us to study the physics of such early times. The figure also shows a depiction of the various new phases one expects to see in the temperature-density phase diagram of QCD. At high enough densities, such as those that exist in very dense stars, the novel phase of colour superconductivity may manifest itself. Whether this can have any observable consequences is a subject of active research as is the subject of investigating the entire phase structure from QCD.

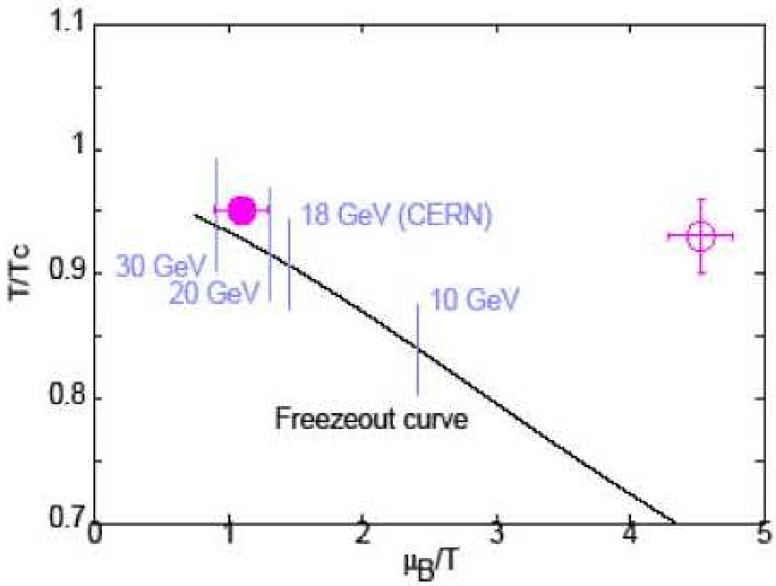

Figure 4. QCD Critical point determinations from two computations with different spatial volumes. The “freezeout curve’ is determined from the experimental results on particle productions.

The lattice technique has led to a prediction that the usual nuclear matter, consisting of protons, neutron, pions etc. undergoes a transition to the new Quark-Gluon plasma state at a temperature $Tc \approx 160$ MeV (about 2 trillion degrees Kelvin). It has also resulted in the equation of state and many other properties, notably the Wroblewski Parameter, shown here on the right from our work

[4]. It is a measure of the production of strange quark-antiquark pairs. It has been proposed as a signal for the new phase, Quark-Gluon Plasma. As one sees in the Figure 3, experiments agree with theoretical (lattice QCD) estimates for the new state. Several other correlations for Heavy Ion Physics have been predicted theoretically in the same way. For instance, lattice QCD also suggests that strangeness is carried by quark-like objects, and supports the idea that flavour in general shows quasi-quark behaviour. The flavour here is a characteristic that separates different type of quarks.

Theoretical physicists, including us [5] have also attempted to look for the critical point in the colourful artistic sketch above. We find it to be located at smaller densities than expected. As shown in the Figure 4, our estimate is that the relativistic heavy ion collider (RHIC), if run at lower colliding energy of about 20-30 GeV, can potentially discover it. Since these collisions take place on a very short time scale, it is a challenging task to look for any signs/imprints of the QCD critical point in their end products. While we shall discuss in more details the experimental aspects of these collisions, let me remark that the basic physics to hunt the QCD critical point is the same as that for usual critical points in the liquid-gas phase diagrams we learn in textbooks, namely critical fluctuations. Any physical quantity displays thermal fluctuations. Indeed, many usual experiments have to be done at very low temperatures to minimize them. In the vicinity of a phase transition or equivalently a critical point the fluctuations become infinitely large. By observing their effects, one hopes to pin down a critical point. Theorists [6] have used lattice techniques to make predictions for such fluctuations. It will be exciting to stack them up against the upcoming experimental results from RHIC and look for the signs of the QCD critical point.

3. HEAVY ION COLLISIONS

Let us now address the questions of where one can find these new phases and whether/how they can be produced in a laboratory. As remarked in the beginning, our Universe was full of QGP at about 10-20 s after the the Big Bang. However, our best chance of studying the Quark-Gluon Plasma is in re-creating that instant of Big Bang. It turns out that the necessary conditions for QGP production in a laboratory are, 1) high energy density, 2) large system size and 3) production of many particles. Heavy ion collisions at velocities $99.5 - 99.995\%$ that of light, possible at the colliders in CERN, Geneva and BNL, New York, indeed meet these conditions. How this happens [1] is schematically illustrated in the left panel of Figure 5. The fireball of QGP condenses into hadrons in extremely short duration of almost an instant. One is forced to sift though the products of the collision in order to establish that QGP was indeed formed. This needs clever detective work. As the right panel of Figure 5 shows, the similarity of the cooling of this fireball produced in heavy ion collisions with the Early Universe can be exploited to devise tools for this task of looking for the new phase QGP. One such tool is jet quenching. It is well known that rare high energetic scatterings of quarks and gluons in the colliding hadrons produce jets of particles. Such jets have been widely studied in proton-proton and electron-positron collisions. If Quark-Gluon Plasma interacts with such a jet, it causes a loss of energy due to multiple scatterings. Since these jets emerge back-to-back due to momentum conservation, only one of them will be seen with the other missing (or extinguished) due to QGP. Such jet quenching has been observed rather extensively. Moreover, an on-off test has been also performed by comparing the collisions of heavy-heavy nuclei, where QGP is expected to be formed, with light-heavy or light-light, where it is not. The latter two were found to have both the jets intact and furthermore these were always back-to-back, as expected. The jet got quenched only in the case where QGP was expected to be formed.

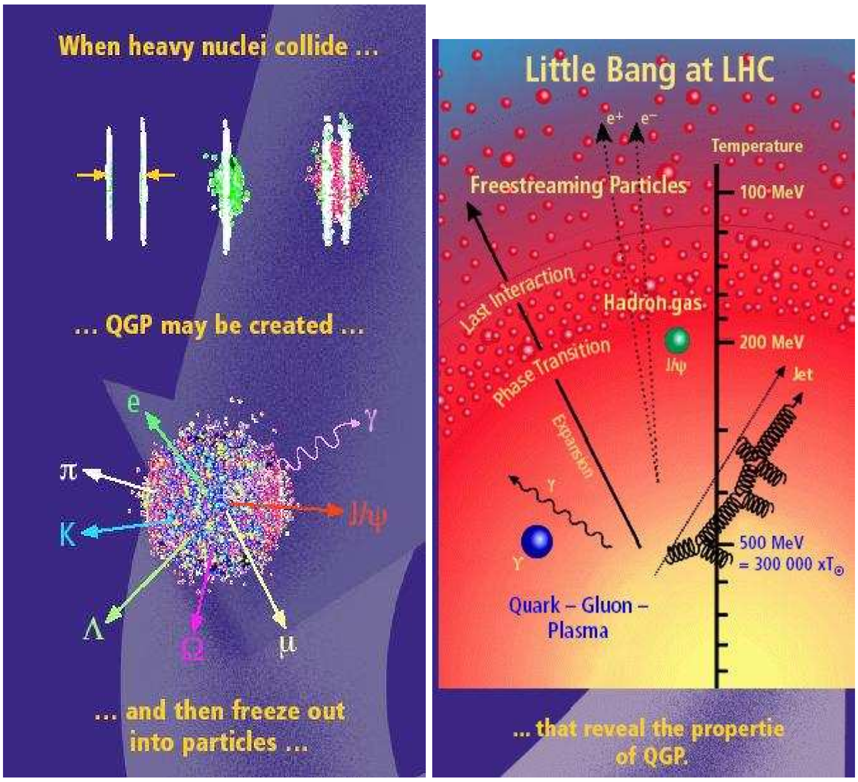

Figure 5. Pictorial representation of heavy ion collisions explaining plasma formation and evaporation (left) and possible signatures of the plasma (right).

Additional evidence for QGP has also been found by looking for the flow in transverse directions which suggests that QGP flows as a perfect liquid with essentially no viscosity. Debye screening, characteristic of plasma, can stop quarks from binding in to hadrons. Anomalous suppression of heavy particles called, J/Ψ, has shown that such Debye screening may have been present in the aftermath of heavy ion collisions. Thus one has tell-tale signs of the new phase Quark-Gluon Plasma having been produced in these collisions.

4. SUMMARY

Lattice QCD predicts new states of strongly interacting matter and is able to shed light on the properties of the Quark-Gluon plasma (QGP) phase. Our results on strangeness production are consistent with the expectation of formation of QGP in experiments. We found that correlations of quantum numbers suggest QGP to have quark-like excitations. Heavy Ion Collisions in CERN Geneva, and BNL, New York, have produced tell-tale signatures of QGP. Many surprises have already been produced by the data and more excitement is likely to come in the upcoming Large Hadron Collider in CERN, Geneva.

References

[1] See e.g., G. Boerner, "The Early Universe: Facts and Fiction", Springer, 2012; E. Kolb and M. Turner, "The Early Universe", Westview Press, 1994.

[2] Mather et al., Astrophysical Journal, 420 (1994) 439, Wright et al., Astrophysical Journal, 420 (1994) 450 and Fixsen et al. Astrophysical Journal, 473 (1996) 576; Simpler description can be found in http://en.wikipedia.org/wiki/CosmicBackgroundExplorer.

[3] J. Cleymans, R. V. Gavai and E. Suhonen, Physics Reports 130 (1986) 217; Helmut Satz, "Extreme States of Matter in Strong Interaction Physics", Springer,2012; K. Yagi, T Hatsuda and Y. Miake, "Quark-Gluon Plasma: From Big Bang to Little Bang", Cambridge University Press, 2005.

[4] R. V. Gavai and S. Gupta, Physical Review D65 (2002) 094515 and Physical Review D73 (2006) 014004.

[5] R V Gavai and S. Gupta, Physical Review D71 (2005) 114014 and Physical Review D78 (2008) 114503.

[6] R V Gavai and S. Gupta, Physics Letters B696 (2011) 459.

Diffusion Dynamics of $ZnCl_2$ in Water by Laser Beam Deflection Method

Sukrutha. K.T. ***, Sasikumar P.R.**†
* M.Sc. Physics (Fourth semester), Maharajas College, Kochi 682 011, India
† Associate Professor (Physics), Maharajas College, Kochi 682 011, India

Abstract. Diffusion is an important phenomenon of scientific and technological interest and recently investigations on diffusion of many chemicals, nano-particles, proteins, drugs etc. in liquids is a thrust area of research. This paper presents a study of temporal and spatial dependence of diffusion of zinc chloride in water by laser beam deflection (LBD) method. When light is passed through a medium of varying refractive index the path of the beam will deflect. A region of refractive index gradient (RIG) is created by carefully mixing sample solution in water with a sharp boundary between the two solutions in a rectangular glass cell of volume about 50cc. Diffusion of one liquid into the other lead to a concentration gradient, which results a spatially and temporally varying RIG. Light from a He-Ne laser, after producing a fan of ray using a cylindrical lens, is passed through the mixing zone in the liquids so that the refracted rays give the LBD pattern, which is collected on a screen. The LBD pattern transformed to a Gaussian profile, the half width at half maximum is related to the diffusion coefficient. The value of diffusion coefficient of zinc chloride solution in water obtained is $1.92 \times 10^{-4} cm^2/sec$.The method can be used to determine the diffusion coefficient of many other materials.

Communicated by: K.C. Ajith Prasad

1. INTRODUCTION

The propagation of an optical beam through a medium characterized by spatial and temporal variation of refractive index is perhaps one of the most widely discussed topic in optical science. Characteristics of such a medium will give valuable information regarding transport and optical properties within the medium. When a light beam is passed through a material having uniform refractive index, the beam will travel along a straight path. If the medium has a varying refractive index, the beam bends in the direction of greater refractive index. Such a deflection in liquid medium can be observed, if there is a refractive index gradient (RIG) in the liquid medium.

2. RIG IN LIQUIDS

In liquids, refractive index gradient can be produced by mixing two miscible liquids of different refractive indices or by mixing same liquids of different concentrations[1-3]. The index of refraction of a solution is approximately proportional to its concentration; hence the gradient of refractive index is proportional to the gradient of concentration. Here the formation of RIG is mainly by diffusion of one liquid to the other.Diffusion, the stochastic motion of particles, tends to establish a uniform concentration. If a concentration gradient is established then diffusion broadens and lowers the concentration gradient over time. Consider two miscible fluids A and B superposed vertically in a cell diffuse in course of time. At time t=0, we deposit a thick layer of B on top of A. The lighter liquid B is put over the heavier one A(Figure 1).The time evolution of density, between two miscible liquids in the separating region give rise to a vertical gradient of refractive index.

3. LASER BEAM DEFLECTION IN LIQUIDS

Laser beam deflection (LBD) technique is an effective and sensitive method for studying the refractive index gradient created in a medium by various causes like temperature and concentration variation. In this method a laser beam with a Gaussian profile is allowed to pass through the interface region, in which the refractive index gradient has been created by diffusion of liquid into water. The amount of deflection suffered by the laser beam is a direct measure of the RIG that has been caused in the defined region and hence yields the value of the parameters of the physical processes that creates the RIG. The method can be used to study the variation of the diffusion coefficient with concentration in liquid. The high accuracy is a result of the fact that no sampling is required and that a large number of transient measurements can be made. In LBD it is possible to determine the diffusing properties in the diffusing medium simultaneously at various special points. This will help to identify the presence of any spatial anisotropy in the medium. The successful determination of diffusion coefficient demonstrates that this technique could be used in practice for the measurement of diffusivity in many chemically and biologically important solutions including nano fluids.

In the case of electrolytic solutions, diffusion co-efficient (D) depends on concentration. The diffusion equation can be written as [4,5],

$$\frac{\partial c}{\partial t} = D(c)\frac{\partial^2 c}{\partial y^2} \tag{1}$$

For low concentration, which corresponds to concentration independent case, it can be treated this equation for the following initial conditions, at time t=0 satisfies a step like concentration as,

$c = c_0$ For $y < 0$

$c = 0$ For $y > 0$

A solution with above distribution can be realized by carefully taking a salt solution of higher refractive index at a known concentration c_0 in the region $y < 0$ and water lower refractive index for $y > 0$. The diffusion of solution in water will develop a gradient RIG formation as a result of concentration variation. As time evolves the concentration gradient disappears and this will result in the broadening of the Gaussian function. Taking above step like initial concentration the variation of concentration at particular intervals is given by [6]

$$\left(\frac{dc}{dy}\right)_t = -\frac{c_0}{\sqrt{4\pi Dt}} exp\left(\frac{-y^2}{4Dt}\right) \tag{2}$$

This is a Gaussian function and will be of the same shape traced out by the deflected beam at the boundary. The half width of the curve at a maximum of dc/dy is measured for a particular time. A graph is plotted between $y_{1/2}^2$ and t the slope of which is $4Dlog_e 2$ and hence, the diffusion coefficient D can be calculated using

$$D = \frac{y_{1/2}^2}{4tlog_e 2} \tag{3}$$

4. EXPERIMENTAL SET-UP

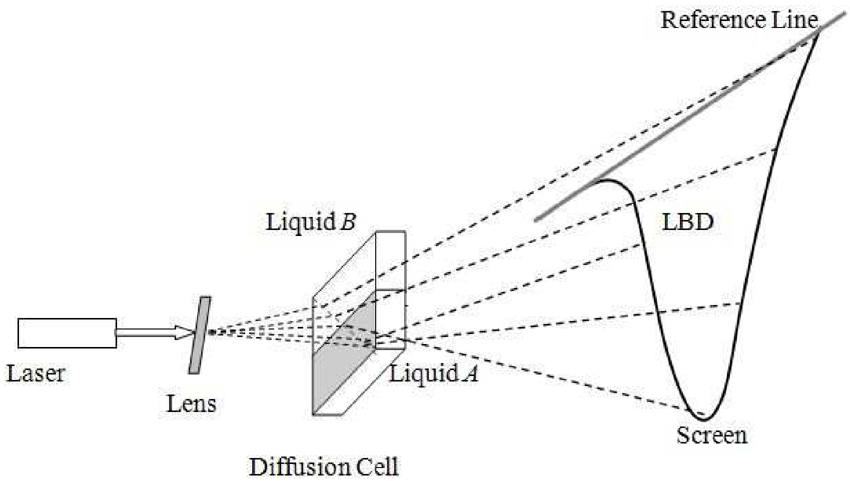

Figure 1. Experimental arrangement for LBD

The basic theory of the method is the deflection of light beam when it passes through a medium having concentration gradient. Rectangular cell is placed at a suitable height. A glass rod about 0.5cm radius mounted at 45^o with respect to the vertical can be used in place of cylindrical lens so as to get a large range of fanned light from a He-Ne laser of wavelength 632.8nm. Take 20ml of water and pipette 20ml of experimental solution in to cell with no random region separating the liquids. The laser beam is deflected at the interface and the deflected beam can be obtained on the screen. The emerging fan of rays then passes through the rectangular diffusion cell in which the two liquids were diffusing into each other across a horizontal miscible interface and allow falling

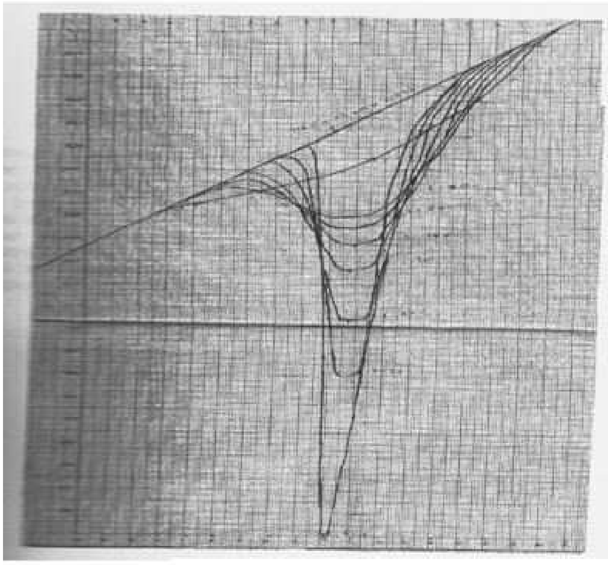

Figure 2. LBD pattern of $ZnCl_2$ in water at different time (bottom t=0 second then after 30 minutes).

diagonally on the screen. In the absence of liquid in the cell, the cylindrical lens produces a straight line image on a screen kept nearly 1.5m away from the cell. The straight line image will be modified when one takes the solution in the cell with concentration gradient due to deflection of light beam resulting from local variation of density and hence the refractive index.Adjust distance between the cell and screen to about 1.5m. The experimental arrangement is shown in Figure 1. Adjust the inclination of the glass road, if necessary, to set this line at 45^o to the vertical. To start the experiment pours the lighter liquid (water) in to the cell and equal amount of denser liquid ($ZnCl_2$) is pipette to the bottom of the cell, in order to minimize the initial mixing of the liquid. The fanned out laser beam is deflected at the interface and the image of the deflected beam is obtained on the screen kept at a distance from the cell. The image of the scattered beam is traced out on a graph paper(Figure 2). The observations are made for various time t and concentrations. The experimental curves of dc/dy versus y obtained at various time intervals from which the half width of the curve at a half maximum is found. It is then plotted (Figure 3) against time and the slope is evaluated and D is calculated using equation (3).

5. RESULTS AND DISCUSSIONS

Studies on diffusion in $ZnCl_2$ solution were carried out by LBD technique with concentrations 8.177g/20ml. In the present work, laser beam deflection in $ZnCl_2$ solution is investigated. The diffusion coefficient of $ZnCl_2$ solution in water and the shift of the LBD peaks are studied. The value

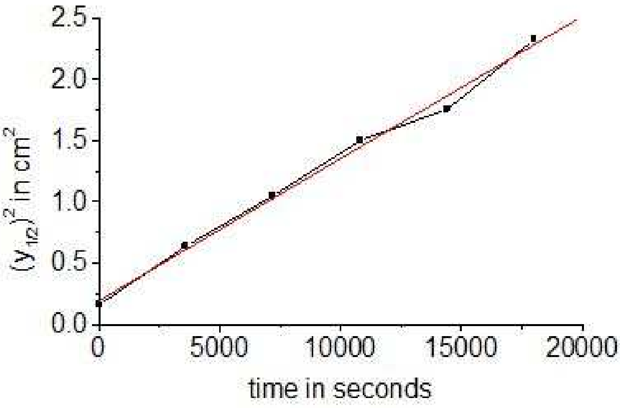

Figure 3. Plot of $y^2_{1/2}$ as a function of t

of diffusion coefficient of $ZnCl_2$ solution is obtained as D=$1.92 \times 10^{-4} cm^2/sec$. The maximum deflection point shifts towards the left where the concentration gradient is the highest. The area enclosed by the LBD image decreases as time progresses and the deflection suffered by the laser beam in the solution varies exponentially with time which can be utilized to investigate the diffusion mechanism of the solution.

ACKNOWLEDGEMENT

Authors are grateful to Directorate of Collegiate Education, Govt. of Kerala, Trivandrum, University Grants Commission, New Delhi and Mahatma Gandhi University, Kottayam for supports.

References

[1] Barnard AJ and Ahlborn B, Am.J.Phys. 43 (1975) 573.
[2] Rashidina N, Balasubramaniam R, Kuang J, Petitjeans P and Maxworthy T Int.J.ThermoPhys. 22(2011) 547.
[3] Rodrigo Riquelme, Ignacio, Carlos Perez-Lopez, Juan A Rayas and Ramon Rodriguez-Veral, J.Phys D Appl.Phys 40(2007) 2769.
[4] CadvidAandGarzonRev.Col.Fis 43(2011) 507.
[5] Andreas Mandelis, Ryoichi Takaue, Zhuohui Chen, Joanna Szurmak and Douglas Baines W Anal.Sci 8 (1992) 131.
[6] Francini F, BuahBassuh P K and Arecchi F T Opt. Commn. 105 (1994) 285.

Interpolating Solution in a Mechanical Model under Quench

Preeti Sahu
School Of Physical Sciences (IInd Year), NISER, Bhubaneswar 751 005, India

Communicated by: L. Satpathy

1. INTRODUCTION

Simple mechanical models often provide insights into complicated physical processes in nature. Consider, for example, phase transition of ferromagnets above the Curie temperature. Below the Curie temperature, within the material, neighbouring magnetic spins are aligned parallel. As we increase the temperature towards the Curie point, the alignment (magnetization) within each domain decreases. Above the Curie temperature, the local magnetic dipoles are randomly oriented and therefore the material behaves as a paramagnet. Theoretical understanding of this phenomenon, including the system's behaviour at the Curie point requires the use of sophisticated techniques of field theory and renormalization group. One may inquire if there exists simple models which capture, at-least qualitatively, some essential features of this transition.

Indeed in [1], such a model was analyzed. It consists of a bead of mass m moving freely along a vertical loop. The loop is then made to rotate about a vertical axis passing through its center. It can be shown that if the loop rotates with a very small angular velocity ω, the bead stays at the bottom of the loop. However, as the angular velocity is increased, beyond a critical velocity ω_c, minimization of the potential energy requires the bead to sit at a non-zero θ (θ is shown in the figure). As we further increase ω, θ increases, reaching $\pi/2$ with $\omega \to \infty$. Note that the symmetry $\theta \to -\theta$, which was present initially, is spontaneously broken for $\omega > \omega_c$ by the equilibrium position of the bead. Similarities with ferromagnetic transition is now immediate. While the role of the temperature is played by the angular velocity ω, the position of the bead θ behaves similar to the order parameter, magnetization. Hence, the paramagnetic phase is analogous to the $\omega < \omega_c$ phase of the model. In literature this phenomena is known as a bifurcation. When a specific physical parameter crosses a threshold value, the system generally organizes itself to a new stable state causing a bifurcation from the original one.

What happens in ferromagnetic material if we quench the temperature from a low value to a value above the Curie temperature? Since temperature is tuned very fast, immediately after the quench, the system will still be in its unstable ferromagnetic state. However, slowly with time, the system will roll down to the stable paramagnetic state. We can ask similar question within the model we are discussing. Suppose we quench the angular velocity from a very low value to a higher one ($> \omega_c$), we should be able to find a time-dependent rolling down solution which will interpolate between $\theta = 0$ and a θ non-zero value. Indeed in [2], such a solution was explicitly constructed.

In this paper, we discuss the same model when it is rotated about a vertical axis *does not* pass through the center. This is explicitly shown in Figure 1. As analyzed in [1], this model depicts some features of ferromagnetic material in an external magnetic field. Here the rotational symmetry is broken by external field itself. Similarly, by choosing off-center axis of rotation, we break the $\theta \to -\theta$ symmetry in our model right from the beginning. We will describe the model in brief in the next section. Our primary aim of this work is to construct explicit rolling down solution as we suddenly shift the axis of rotation of the loop parallely. This is what we discuss in the third section. The last section summarizes the results.

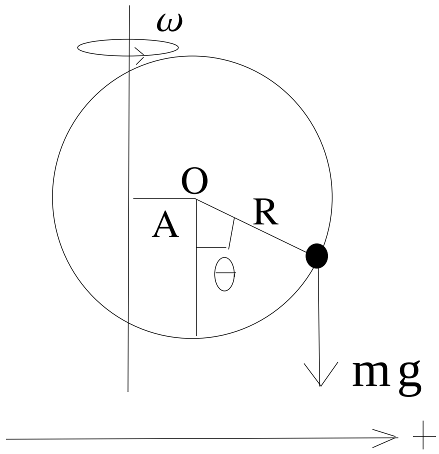

Figure 1. A vertical loop carrying a movable friction-lees bead is rotating about an off-center vertical axis, at a distance A from the center, with a constant frequency ω. The positive values of A and θ are shown by the horizontal axis at the bottom.

2. THE LAGRANGIAN AND THE EQUATION OF MOTION

As discussed in [1], the model has an effective Lagrangian description. Let us assume that at any instant of time the mass is at a position $\theta(t)$ The Lagrangian then reads [1]

$$L = \text{kinetic energy} - \text{potential energy}. \tag{1}$$

While the kinetic energy is given by

$$KE = \frac{1}{2}mR^2\dot{\theta}^2 + \frac{1}{2}m\omega^2(R\sin^2\theta + A)^2, \tag{2}$$

the potential energy is

$$PE = -mgR\cos\theta. \tag{3}$$

Therefore the total Lagrangian is

$$L = \frac{1}{2}mR^2\dot{\theta}^2 + \frac{1}{2}m\omega^2(R\sin^2\theta + A)^2 + mgR\cos\theta. \tag{4}$$

This allows us to have a description of the system in terms of an *effective* potential

$$V' = -\frac{1}{2}m\omega^2(R\sin^2\theta + A)^2 - mgR\cos\theta. \tag{5}$$

Or, in other words, we can study the equilibrium position of the bead by analyzing the minima of the potential

$$V = \frac{V'}{mgR} = -\cos\theta - \frac{1}{2}(\sin\theta + \alpha)^2, \tag{6}$$

where we have defined

$$\alpha = \frac{A}{R}, \quad \text{and} \;\; \beta = \frac{\omega^2 R}{g}. \tag{7}$$

Note that, because of the presence of α, the potential does not have a $\theta \to -\theta$ symmetry.

In the following, we will study the effective potential in the range $\beta > 1$ and for all positive α. Notice that, for $\alpha = 0$, it has a maximum at $\theta = 0$ with two symmetric minima at

$$\theta_0 = \pm\cos^{-1}(1/\beta). \tag{8}$$

Let the bead be in one of the degenerate minima. We choose the negative one. Now we increase α. This means that, in Figure (1), we move the axis of rotation to the right. For very large α, we can neglect the $\sin\theta$ term in the potential. It then easily follows that there is only one minimum at approximately

$$\theta = \tan^{-1}(\beta\alpha) \tag{9}$$

So at this high α, the bead must be resting at a positive θ value. To find at what value of α, the transition from negative to positive θ occurred, it is instructive to search if there is an inflection point associated with the effective potential. Indeed there is one and that can be found by setting first and second θ derivative to zero. It occurs at

$$\alpha = \alpha_c = (1 - \beta^{-2/3})^{3/2}, \;\; \cos\theta_c = \frac{1}{\beta^{1/3}} \tag{10}$$

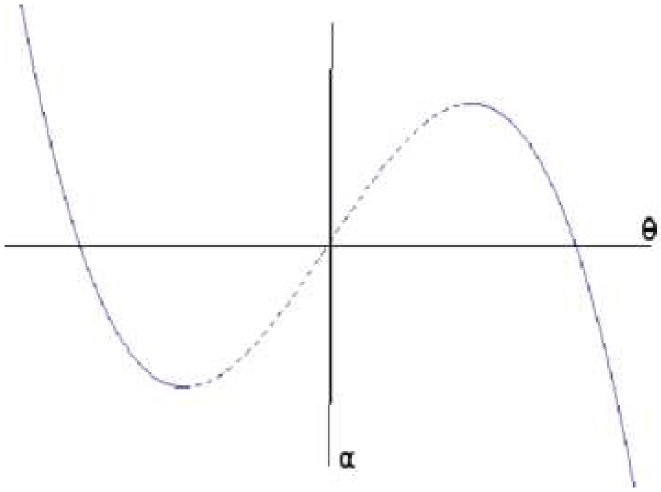

Figure 2. Bifurcation Diagram for the model. The dotted lines show the points of unstable equilibrium; whereas the solid lines represent points of stable equilibrium. As soon as α is slightly decreased from the maximum (call it α_c) – which is the transition point with saddle-point bifurcation –, the particle sitting on the left false vacua, should slip down to the true vacuum at the right.

The dependence of equilibrium angle on alpha is shown in Figure 2 by a bifurcation diagram [4]. Further, the behaviour of the potential is shown in Figure 3.

Now we would like to address the following question. Suppose, for a fixed β, we suddenly change α from a value less then α_c to a value greater than α_c, how is the bead going to relax from a wrong ground state (at negative θ) to the right one (in positive θ)? To address this question, we need to find out a rolling down solution of θ as a function of *time*. We address this issue in the next section.

3. INTERPOLATING SOLUTION

We start with by writing down the Euler-Lagrange equation that follows from (4). This is given by

$$\frac{d^2\theta}{dt^2} - \omega^2 \sin\theta \cos\theta - \frac{\omega^2 A}{R} \cos\theta + \frac{g}{R} \sin\theta = 0 \tag{11}$$

By defining $\tilde{t} = \omega t$, we can re-write the equation as

$$\frac{d^2\theta}{d\tilde{t}^2} - \sin\theta \cos\theta - \alpha \cos\theta + \frac{1}{\beta} \sin\theta = 0. \tag{12}$$

Integrating this equation once, we get

$$\frac{1}{2}\left(\frac{d\theta}{d\tilde{t}}\right)^2 + \frac{1}{4} \cos 2\theta - \alpha \sin\theta - \frac{1}{\beta} \cos\theta = c, \tag{13}$$

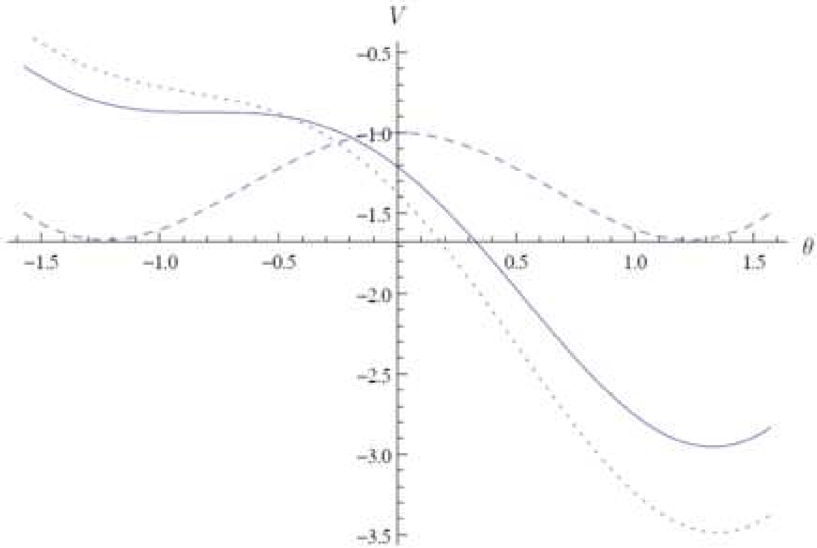

Figure 3. Effective potential for fixed $\beta = 3$ and for various α. For $\alpha = 0$ (dashed line), there are degenerate minima. The solid line is for $\alpha = \alpha_c = (1 - \beta^{-2/3})^{3/2} = .374$ which shows the inflection point arising from the left minimum. For $\alpha = .5$, single minimum is shown by the dotted line.

where, c is an integration constant to be determined by the boundary condition. Note that the above equation is just a statement of energy conservation.

To this end, let us consider the following situation. Suppose we start with $\alpha = 0$ and $\beta > 1$. The particle is sitting in one of the degenerate minima given by

$$\theta_+ = \cos^{-1}\left(\frac{1}{\beta}\right), \text{ or } \theta_- = 2\pi - \cos^{-1}\left(\frac{1}{\beta}\right). \tag{14}$$

Let us take the second one. Now we suddenly increase α to a value greater than α_c. Since θ_- is no longer a minimum of the effective potential, particle is expected to roll down from its unstable position with zero initial velocity. This condition allow us to fix the constant appearing in (13).

$$\frac{d\theta}{d\tilde{t}} = 0, \quad \text{at } \theta = \theta_-, \tag{15}$$

With this value of the constant, one can search for a time dependent solution for θ simply by integrating (13). This exercise can be performed exactly, but the solution is a bit messy. We rather illustrate here with specific values of β and α. Let us choose $\beta = 3$. Using (10), we get $\alpha_c = .3742$. We therefore take $\alpha = .375$. With this the boundary condition can be solved to get $c = 0.0472$. Now the equation (13) can be re-written as

$$\int \frac{d\theta}{\sqrt{2\alpha\,\sin\theta + 2/\beta\,\cos\theta - \cos 2\theta/2 + 2 \times .0472}} = \pm \int d\tilde{t}. \tag{16}$$

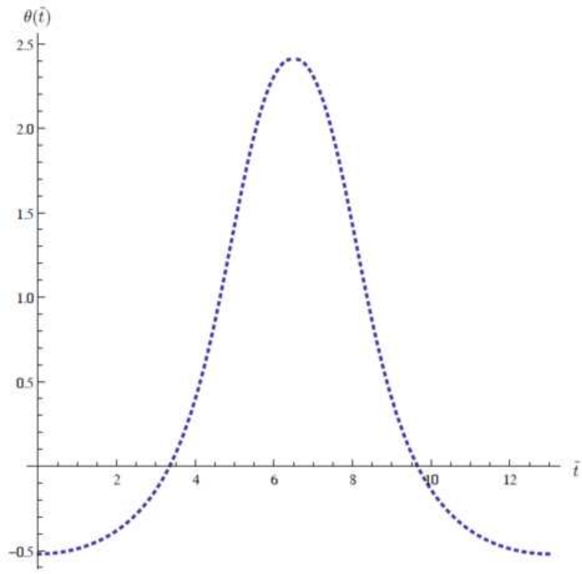

Figure 4. Behaviour of $\theta(\tilde{t})$ with $\tilde{t}$ for $\alpha = .375$ where $\alpha_c = .3742$. We have set $\beta = 3$. The figure, which would correspond to a bounced like solution in Euclidean time, is seen as an interpolating one in real time.

The integral on the left hand side of (16) can be solved. However, but again the result is not very illuminating. We instead represent the solution graphically. This is shown in Figure 4.

4. SUMMARY

To conclude, in this paper, we reviewed a toy model which captures certain qualitative behaviour of a ferromagnet as we tune its temperature in the presence of an external magnetic filed. We then constructed a time-dependent classical solution representing its relaxation from false to a true ground state after the model is appropriately quenched.

ACKNOWLEDGEMENTS

This work is done under supervision of Sudipta Mukherji, Institute of Physics, Bhubaneswar.

References

[1] G. Fletcher, Am. J. Phys. 65, (1997) 1.
[2] S.S. Mishra, Prayas: Students' Journal of Physics 4, (2010) 17.
[3] S. Kar and A. Khare, Am. J. Phys. 68, (2000) 1128.
[4] Steven H. Strogatz, *Non Linear Dynamics and Chaos*.

An Alternative Derivation of Thomas Precession Effect

Mritunjay Kumar Verma*
Centre For Basic Sciences, Kalina, Santacruz (E), Mumbai University, Mumbai 400098, India

Abstract. In this article, we present an alternative derivation of the Thomas precession effect. The derivation follows from a method of generalization of inertial forces to relativistic domain given by H. Nikolić. The basic method employed is to sum infinitesimal Lorentz transformations to arrive at the metric tensor for an accelerating observer (in flat space-time). Using this in the geodesic equation gives the equation of motion of a free particle in a (non inertial) accelerated frame in flat space-time. This equation has the correct Newtonian limit and gives the desired expression for the Thomas precession.

Communicated by: D.P. Roy

1. INTRODUCTION

In Newtonian mechanics, the inertial forces (i.e. forces of kinematic origin), acting on a particle for a non-inertial observer are well known. However, Newtonian mechanics is valid only in the limit of speeds low compared to the speed of light c. It is a limiting case of Einstein's special relativistic mechanics. So, a natural question to ask is how the inertial forces of Newtonian mechanics are generalized to the relativistic domain. This question is quite non-trivial and in this article, we present in detail one approach due to H. Nikolić (2004) to arrive at the relativistic form of inertial forces that in the low speed limit reduce to the known results of Newtonian mechanics. In addition, this generalization reproduces the well known relativistic effect, namely Thomas precession, and thus provides an independent way of arriving at this effect.

This article is organized as follows: in section 2, a summary of inertial forces in Newtonian mechanics is given. Section 3 is devoted to obtain the metric tensor for an accelerating observer in flat space-time. In section 4, we use the metric tensor to obtain the equation of motion of a free particle as seen by the accelerating observer. This equation, as expected, has the correct Newtonian limit. Further, it also contain terms, analogous to the inertial forces for a rotating frame in Newtonian mechanics, with an angular velocity that is the familiar Thomas precession velocity.

*mritunjay@cbs.ac.in

2. INERTIAL FORCES IN NEWTONIAN MECHANICS

As we know, Newton's second law, namely $\vec{F} = m\vec{a}$ (where $\vec{F}$ is a force due to some physical agency) holds true only in inertial frames (defined as a co-ordinate system in which a particle free from all physical interactions moves with a constant velocity). This is the simplest form of equation of motion of a particle. (This is true for any physical law. The laws of nature take their simplest mathematical form in inertial frames). However, if we want to analyze the motion of the same particle from the point of view of a non-inertial observer, a number of additional terms arise and the equation $\vec{F} = m\vec{a}$ gets modified. The origin of these terms is purely kinematical. These additional terms are proportional to inertial mass and are variously called inertial forces, pseudo forces, frame dependent forces, etc.

In Newtonian mechanics, the equation of motion of a free particle for a non inertial observer is well known and is given by

$$\vec{A}\,' = -\vec{a} - \vec{\omega} \times \left(\vec{\omega} \times \vec{x}\,'\right) - 2\left(\vec{\omega} \times \vec{v}\,'\right) - \dot{\vec{\omega}} \times \vec{x}\,' \quad (1)$$

where $\vec{A}\,'$ is the acceleration of the particle as measured by the non inertial observer. $\vec{a}$ and $\vec{\omega}$ are the acceleration and rotational velocity respectively of the non inertial observer. $\vec{v}'$ and $\vec{x}'$ are the velocity and position vector respectively of the particle with respect to the non inertial observer.

The second term on the right hand side, in the above equation, is known as the *centrifugal* term while the third term is known as the *Coriolis* term. The third term is present only when the particle has a non-zero velocity with respect to the the non-inertial observer. The last term vanishes if $\vec{\omega}$ is constant.

In the present article, we give the relativistic generalization of equation (1) for the case of pure translational acceleration, i.e. for $\vec{\omega} = 0$. The general case is considerably more involved and is treated in references [1] and [2]. See also reference [5] which provides this derivation in much detail.

3. METRIC TENSOR OF THE ACCELERATING OBSERVER

We consider an inertial frame S and a non inertial frame S' which has translational acceleration $\vec{a}$ with respect to the inertial frame S. An observer is located at the origin of the non inertial frame. In the approach considered here [1], the calculation of the metric tensor is valid only for the non inertial observer at the origin (this will be clear subsequently in the calculation). For obtaining the equation of motion of a free particle with respect to a non inertial observer however, this is all we require.

The (covariant) metric tensor for an observer in S is the standard metric of special relativity given by

$$g_{\mu\nu} = \eta_{\mu\nu} = diag(1, -1, -1, -1) \quad (2)$$

We use the convention that the Greek indices (μ, ν etc.) run over $0, 1, 2, 3$ while the roman indices (i, j etc.) run over $1, 2, 3$ and denote the three spatial components of a vector.

If $g'_{\mu\nu}$ is the metric tensor for the non inertial observer, the two are related by

$$g'_{\mu\nu} = \frac{\partial x^\sigma}{\partial x'^\mu}\frac{\partial x^\rho}{\partial x'^\nu} g_{\sigma\rho} \tag{3}$$

Thus, to compute $g'_{\mu\nu}$, we need the relationship between x^μ and x'^μ i.e. we require co-ordinate transformation equation between these two frames. This transformation is not the familiar Lorentz transformation, which is valid only for two inertial observers in uniform relative motion. Observer in S' is accelerating. So we need to generalize the Lorentz transformation. This is done in the next subsection.

3.1 *Generalized Lorentz Transformation*

The usual Lorentz transformation between two inertial frames related by a constant relative velocity $\vec{u}$ is given by

$$x^o = \gamma\big(x'^o + \frac{\vec{u}\cdot\vec{x}'}{c^2}\big) \qquad \text{and} \qquad x^i = x'^i + (\gamma - 1)\tfrac{\vec{u}\cdot\vec{x}'}{u^2}u^i + \gamma u^i x'^o \tag{4}$$

where a given event has co-ordinates (x^o, x^i) with respect to S and co-ordinates (x'^o, x'^i) with respect to S' and $\gamma = \frac{1}{\sqrt{1-\frac{u^2}{c^2}}}$.

Equation (4) gives the Lorentz transformation in which the velocity $\vec{u}$ of S' relative to S is along an arbitrary direction (the axes of S and S' are however parallel).

Let, $x^\mu = f^\mu(x'^o, \vec{x}'; \vec{u})$ denote the above Lorentz transformation for constant relative velocity $\vec{u}$.

Transition to the non inertial frame S' introduces a time dependent velocity: $\vec{u} \to \vec{u}(x^o) = \vec{u}(x'^o, x'^i) = \vec{u}(x'^o)$ (since $x'^i = 0$ for the observer at origin) in which case transformation between S and S' is not given by equation (4). However, the required transformation between S and S' can be obtained by summing the infinitesimal Lorentz transformation given by the differential

$$dx^\mu = \left(\frac{\partial f^\mu}{\partial x'^\nu}\right)dx'^\nu = f^\mu_\nu(x'^o, \vec{x}'; \vec{u})dx'^\nu \tag{5}$$

where,

$$f^\mu_\nu = \left(\frac{\partial f^\mu}{\partial x'^\nu}\right)_{\vec{u}=constant}$$

Using equation (4), we obtain

$$f^o_o = \gamma, \qquad f^o_j = \frac{-\gamma u_j}{c}, \qquad f^i_o = \frac{\gamma u^i}{c}, \qquad \text{and} \qquad f^i_j = \delta^i_j + \frac{1-\gamma}{u^2}u^i u_j$$

We can integrate equation (5) to get the relation between x^μ and x'^μ. We integrate the equation from $x'^\mu = (0,0)$ to $x'^\mu = (x'^o, x'^j)$. This is done as follows

$$x^\mu = \int_o^{x'^o} f_o^\mu(x''^o, o; \vec{u}(x''^o))dx''^o + \int_C f_k^\mu(x'^o, \vec{x}'; \vec{u}(x'^o))dx'^k \tag{6}$$

Since dx^μ is an exact differential, the integration will give the same answer whatever path we choose between the end points. So, for convenience we choose a path which has two segments. Along the first segment, $x'^i = 0$, and only temporal component x'^o varies from 0 to x'^o. Along the second segment, we take x'^o = constant and vary space variable x'^k from 0 to x'^j along an arbitrary spatial curve C. The advantage of choosing this path of two segments is that time and space integrations separate out and integration of equation (5) becomes tractable.

Using equation (6), and the fact that spatial integration varies from $x'^k = 0$ to $x'^k = x'^j$ we obtain

$$\begin{aligned} x^\mu + \Delta x^\mu &= \int_0^{x'^o + \Delta x'^o} f_o^\mu(x''^o, 0; \vec{u}(x''^o))dx''^o \\ &+ \int_0^{x'^j + \Delta x'^j} f_k^\mu\big(x'^o + \Delta x'^o, \vec{x}'; \vec{u}(x'^o + \Delta x'^o)\big)dx'^k \end{aligned} \tag{7}$$

We can expand various terms in second integral in the right hand side in a Taylor series to first order as

$$\begin{aligned} f_k^\mu(x'^o + \Delta x'^o, \vec{x}'; \vec{u}(x'^o + \Delta x'^o)) &\approx f_k^\mu(x'^o, \vec{x}'; \vec{u}(x'^o)) + \frac{\partial f_k^\mu(x'^o, \vec{x}'; \vec{u}(x'^o))}{\partial u^l}\Delta u^l \\ &= f_k^\mu(x'^o, \vec{x}'; \vec{u}(x'^o)) + \frac{\partial f_k^\mu(x'^o, \vec{x}'; \vec{u}(x'^o))}{\partial u^l}\frac{\partial u^l}{\partial x'^o}\Delta x'^o \end{aligned}$$

where we have taken into account the fact that f_k^μ does not depend explicitly on time variable x'^o but depends only implicitly through $\vec{u}$.

Noting the limit points in equation (6), we subtract the equation (6) from (7). In the limit $\Delta x'^o, \Delta x'^i \to 0$, we obtain

$$\Delta x^\mu = f_o^\mu \Delta x'^o + \frac{\partial u^l}{\partial x'^o} x'^j \frac{\partial f_j^\mu}{\partial u^l}\Delta x'^o + f_j^\mu \Delta x'^j$$

We note from the above equation that time coordinates of S and the S' observer at the origin (so that x'^i =0) are related by $t = \gamma t'$ and hence for the observer at the origin,

$$\frac{\partial u^l}{\partial x'^o} = \frac{1}{c}\frac{\partial u^l}{\partial t'} = \frac{1}{c}\frac{\partial u^l}{\partial t}\frac{\partial t}{\partial t'} = \frac{\gamma}{c}\frac{\partial u^l}{\partial t} = \frac{\gamma}{c}a^l$$

where $a^l = \frac{\partial u^l}{\partial t}$ is the acceleration of the S' observer with respect to the S frame. Using this, we obtain

$$\Delta x^\mu = f_o^\mu \Delta x'^o + \frac{\gamma}{c}a^l x'^j \frac{\partial f_j^\mu}{\partial u^l}\Delta x'^o + f_j^\mu \Delta x'^j \tag{8}$$

This gives the desired co-ordinate relationship between the two frames. This can be used to compute the various partial derivatives needed to compute the metric tensor in equation (3). The final results are given below

$$
\begin{aligned}
&1. \quad \frac{\partial x^o}{\partial x'^j} = -\frac{\gamma}{c}u_j \\
&2. \quad \frac{\partial x^i}{\partial x'^j} = \delta^i_j \; + \; \frac{1-\gamma}{u^2}u^i u_j \\
&3. \quad \frac{\partial x^o}{\partial x'^o} = \gamma \; - \; \frac{\gamma^2}{c^2}a_i x'^i \; + \; \frac{\gamma^4}{c^4}a^k u_k u_i x'^i \\
&4. \quad \frac{\partial x^k}{\partial x'^o} = \; \frac{\gamma}{c}u^k - \frac{\gamma(\gamma-1)}{u^2 c}a^k u_j x'^j - \frac{\gamma(\gamma-1)}{u^2 c}a_j u^k x'^j \\
&\qquad\qquad + \frac{\gamma^4}{u^2 c^3}a^l u_l u^k u_j x'^j - \frac{2\gamma(\gamma-1)}{u^4 c}a^l u_l u^k u_j x'^j
\end{aligned}
\tag{9}
$$

3.2 *Metric Tensor*

Metric tensor for S' observer can now be computed using equation (3) and the various partial derivatives as computed in previous subsection. The calculations are straightforward but rather lengthy, so only the results are given here.

$$
\begin{aligned}
&1. \quad g'_{ij} = -\delta_{ij} \\
&2. \quad g'_{oj} = g'_{jo} = \frac{\gamma}{c}(\vec{\omega}_{\rm T} \times \vec{x}')_j \\
&3. \quad g'_{oo} = \big(1 + \frac{\vec{a}' \cdot \vec{x}'}{c^2}\big)^2 - \frac{\gamma^2}{c^2}(\vec{\omega}_{\rm T} \times \vec{x}') \cdot (\vec{\omega}_{\rm T} \times \vec{x}')
\end{aligned}
\tag{10}
$$

where, $a'^i = \gamma^2[a^i + \frac{1}{u^2}(\gamma-1)(\vec{u}\cdot\vec{a})u^i]$ and $(\omega_{\rm T})_i = \frac{1}{2u^2}(\gamma-1)\epsilon_{ijk}(u^j a^k - u^k a^j)$ $\vec{\omega}_{\rm T} = \frac{\gamma-1}{u^2}(\vec{u}\times\vec{a})$ will be later interpreted as the Thomas precession frequency. It is clear that the metric given above reduces to the usual inertial frame metric dig(1,-1,-1,-1) when acceleration is zero.

Note that for the special case when $\vec{a}$ is parallel to $\vec{u}$, $\vec{\omega}_{\rm T} = 0$ and the metric above coincides with the well known metric for a linearly accelerated observer (see, for example, reference [4])

$$ds^2 = c^2\big(1 + \frac{\vec{a}' \cdot \vec{x}'}{c^2}\big)^2 dt^2 - dx^2 - dy^2 - dz^2$$

Here $\vec{a}'$ is the proper acceleration of the non inertial observer. It is straightforward to show that this interpretation of $\vec{a}'$ is true even when $\vec{a}$ is not parallel to $\vec{u}$ [2].

4. GEODESIC EQUATION

Geodesic equation describes the path followed by a particle which is moving freely. One can think of the geodesic equation as the generalization of Netwon's force free motion $\frac{d^2x^i}{dt^2} = 0$. Unlike Newton's equation, geodesic equation is valid for a general coordinate system not necessarily an inertial one. Various terms appearing in the equation of motion can be interpreted as the inertial forces acting on the particle.

The geodesic equation in any co-ordinate system for a particle, moving freely, is given by

$$\frac{d^2x^\mu}{d\tau^2} + \Gamma^\mu_{\sigma\rho}\frac{dx^\sigma}{d\tau}\frac{dx^\rho}{d\tau} = 0 \tag{11}$$

where x^μ is the space-time co-ordinate of the particle with respect to the observer and τ is the proper time measured by a clock moving with the particle (τ is used as a parameter to parametrize the curve in space-time (world-line) along which the particle is moving). $\Gamma^\mu_{\sigma\rho}$ is known as the Christoffel symbol of second kind.

Now, τ is the time measured by the clock moving with the particle. But, we want to find the equation of motion as seen by the non inertial observer. Acceleration of the particle can be obtained using the spatial part of geodesic equation. So, we need to write the spatial components of geodesic equation in terms of time measured by S' observer (i.e. $t' = \frac{x'^o}{c}$). This task is achieved by using temporal component of geodesic equation to eliminate τ for t'. This is done in the next subsection.

4.1 *Acceleration of the Particle in Non Inertial Frame*

Our goal is to find an expression for $\frac{d^2x'^i}{dt'^2}$. We proceed as follow:

$$\frac{dx'^\mu}{d\tau} = \frac{dx'^\mu}{dt'}\frac{dt'}{d\tau}$$

$$\Rightarrow \frac{d^2x'^\mu}{d\tau^2} = \frac{d^2x'^\mu}{dt'^2}\left(\frac{dt'}{d\tau}\right)^2 + \frac{dx'^\mu}{dt'}\frac{d^2t'}{d\tau^2}$$

Using this in geodesic equation, we obtain for temporal component

$$\frac{d^2t'}{d\tau^2}\left(\frac{dt'}{d\tau}\right)^{-2} = -\frac{1}{c}\Gamma^o_{\sigma\rho}\frac{dx'^\sigma}{dt'}\frac{dx'^\rho}{dt'}$$

and for spatial component

$$\frac{d^2x'^i}{dt'^2}\left(\frac{dt'}{d\tau}\right)^{-2} = -\frac{dx'^i}{dt}\frac{d^2t'}{d\tau^2}\left(\frac{dt'}{d\tau}\right)^{-2} - \Gamma^i_{\sigma\rho}\frac{dx'^\sigma}{dt'}\frac{dx'^\rho}{dt'}$$

Eliminating $\frac{d^2t'}{d\tau^2}\left(\frac{dt'}{d\tau}\right)^{-2}$ by making use of temporal component, we obtain

$$\frac{d^2x'^i}{dt'^2} = -\frac{dx'^i}{dt}\left[-\frac{1}{c}\Gamma^o_{\sigma\rho}\frac{dx'^\sigma}{dt'}\frac{dx'^\rho}{dt'}\right] - \Gamma^i_{\sigma\rho}\frac{dx'^\sigma}{dt'}\frac{dx'^\rho}{dt'}$$

Expanding various summation terms and making some rearrangement, we finally obtain the desired result

$$\frac{d^2x'^i}{dt'^2} = \left[\frac{1}{c}\Gamma^o_{jk}\frac{dx'^j}{dt'}\frac{dx'^k}{dt'} + 2\Gamma^o_{oj}\frac{dx'^j}{dt'} + c\Gamma^o_{oo}\right]\frac{dx'^i}{dt'} - \left[\Gamma^i_{jk}\frac{dx'^j}{dt'}\frac{dx'^k}{dt'} + 2c\Gamma^i_{oj}\frac{dx'^j}{dt'} + c^2\Gamma^i_{oo}\right] \tag{12}$$

Next, we need to compute various Christoffel symbols for the metric obtained earlier and insert in above equation.

4.2 *Computation of Christoffel Symbols*

Christoffel symbols are defined as

$$\Gamma^\mu_{\sigma\rho} = \frac{1}{2}g^{\mu\lambda}\left\{\frac{\partial g_{\rho\lambda}}{\partial x'^\sigma} + \frac{\partial g_{\sigma\lambda}}{\partial x'^\rho} - \frac{\partial g_{\sigma\rho}}{\partial x'^\lambda}\right\}. \tag{13}$$

Here onwards we use unprimed $g^{\mu\nu}$ to represent $g'^{\mu\nu}$. With that, $g^{\mu\lambda}$ is the contravariant metric tensor given by the inverse of matrix $[g_{\mu\nu}]$ and is computed to be

$$[g^{\mu\nu}] = \frac{1}{g}\begin{bmatrix} -1 & -g_{01} & -g_{02} & -g_{03} \\ -g_{10} & g_{00} + g_{02}^2 + g_{03}^2 & -g_{01}g_{02} & -g_{01}g_{03} \\ -g_{20} & -g_{01}g_{02} & g_{00} + g_{01}^2 + g_{03}^2 & -g_{02}g_{03} \\ -g_{30} & -g_{01}g_{03} & -g_{02}g_{03} & g_{00} + g_{01}^2 + g_{02}^2 \end{bmatrix}$$

where, $\quad g = \det[g_{\mu\nu}] = -g_{00} - g_{01}^2 - g_{02}^2 - g_{03}^2 = -\left(1 + \frac{\vec{a}'\cdot\vec{x}'}{c^2}\right)^2.$

Using the definition (13) and the expression of the metric tensor components (contravariant as well covariant), different Christoffel symbols are computed to be

1. $\Gamma^i_{jk} = 0$
2. $\Gamma^o_{jk} = 0$
3. $\Gamma^o_{jo} = \frac{1}{c^2}\left(1 + \frac{\vec{a}'\cdot\vec{x}'}{c^2}\right)^{-1}a'_j$
4. $\Gamma^i_{jo} = \frac{1}{c}\left[-\gamma\epsilon_{jik}\omega^k_{\mathrm{T}} + \frac{\gamma}{c^2}\left(1 + \frac{\vec{a}'\cdot\vec{x}'}{c^2}\right)^{-1}a'_j(\vec{\omega}_{\mathrm{T}} \times \vec{x}')^i\right]$
5. $\Gamma^o_{oo} = \frac{1}{c^3}\left(1 + \frac{\vec{a}'\cdot\vec{x}'}{c^2}\right)^{-1}\left[-\gamma(\vec{\omega}_{\mathrm{T}} \times \vec{x}')\cdot\vec{a}' + \dot{\vec{a}}'\cdot\vec{x}'\right]$
6. $\Gamma^i_{oo} = \frac{1}{c^2}\Big[-\gamma(\dot{\vec{\omega}}_{\mathrm{T}} \times \vec{x}')^i + \gamma^2\{\vec{\omega}_{\mathrm{T}} \times (\vec{\omega}_{\mathrm{T}} \times \vec{x}')\}^i + \left(1 + \frac{\vec{a}'\cdot\vec{x}'}{c^2}\right)a'^i$
   $+ \frac{\gamma}{c^2}\left(1 + \frac{\vec{a}'\cdot\vec{x}'}{c^2}\right)^{-1}(\vec{\omega}_{\mathrm{T}} \times \vec{x}')^i\left\{-\gamma(\vec{\omega}_{\mathrm{T}} \times \vec{x}')\cdot\vec{a}' + \dot{\vec{a}}'\cdot\vec{x}'\right\}\Big]$

4.3 *Generalization of Inertial Forces and Thomas Precession*

Various Christoffel symbols computed in previous subsection can now be inserted in equation (12) to obtain the acceleration of the particle in terms of dynamical quantities. The final result turns out to be

$$\begin{aligned} A'^i = \frac{d^2x'^i}{dt'^2} = & -\left(1+\frac{\vec{a}'\cdot\vec{x}'}{c^2}\right)^{-1} a'^i + \big(\gamma\dot{\vec{\omega}}_{\rm T}\times\vec{x}'\big)^i \\ & +2\gamma\big(\vec{\omega}_{\rm T}\times\vec{v}'\big)^i - \gamma^2\big\{\vec{\omega}_{\rm T}\times(\vec{\omega}_{\rm T}\times\vec{x}')\big\}^i \\ & +\frac{1}{c^2}\left(1+\frac{\vec{a}'\cdot\vec{x}'}{c^2}\right)^{-1}\Big[2\big(\vec{v}'-\gamma\vec{\omega}_{\rm T}\times\vec{x}'\big)\cdot\vec{a}' + \big(\vec{a}'-\gamma\vec{\omega}_{\rm T}\times\vec{a}'\big)\cdot\vec{x}'\Big] \\ & \Big[v'^i - \gamma\big(\vec{\omega}_{\rm T}\times\vec{x}'\big)^i\Big] \end{aligned}$$

where, $v'^i = \frac{dx'^i}{dt'}$ is the velocity of the particle as measured in the non inertial frame. This is the general equation of motion of a free particle as seen by a non inertial accelerating observer. The various terms multiplied by the inertial mass give the generalized inertial forces in relativistic domain.

It can be noted that the new generalized equation contains many complicated terms. The most important point is that though we took the frame to be accelerating only translationally with respect to the frame S, the inertial forces appearing in the equation are such as if the frame is rotating with angular velocity $-\vec{\omega}_{\rm T}$ (to see this, note the second, third and fourth terms in above equation and compare with equation (1). Also note that these are the only $\vec{\omega}_{\rm T}$ containing terms surviving upto order $\frac{u^2}{c^2}$). Thus, a free particle (which moves uniformly in a straight line in the inertial frame S) in the accelerated frame will experience inertial forces analogous to those experienced in a non relativistic rotating frame, corresponding to a rotation of $-\vec{\omega}_{\rm T}$. This effect is present only when the velocity and the acceleration of the accelerating observer are not collinear (see the definition of $\vec{\omega}_{\rm T}$ just below equation (10)). Provided $\vec{\omega}_{\rm T}$ is non zero, a spin vector in the rest frame precess with respect to the inertial frame S with precessional velocity $\vec{\omega}_{\rm T}$. This effect is known as Thomas precession and is patently a special relativistic effect. The standard derivation of this effect is based on the fact that two Lorentz boosts in arbitrary directions do not commute and are equivalent to another boost plus a rotation [3]. It is interesting to see that a completely different approach, as described in this article, reproduces the same effect.

4.4 *Newtonian limit of equation of motion*

In the Newtonian limit, $c \to \infty$ and $\gamma \to 1$. Various quantities take the limiting form

$$\vec{\omega}_{\rm T} = \frac{\gamma-1}{u^2}(\vec{a}\times\vec{u}) \to 0$$

$$\vec{a}' = \gamma^2\Big[\vec{a} + \frac{\gamma-1}{u^2}(\vec{u}\cdot\vec{a})\vec{u}\Big] \to \vec{a}$$

Also, all terms containing $\frac{1}{c^2}$ drop out. Hence, in the Newtonian limit, acceleration of the particle in non-inertial frame takes the form-

$$\vec{A}\,' = -\vec{a}$$

This matches with the Newtonian result (1) for the case when rotational velocity $\vec{\omega}$ of the non inertial observer is zero.

5. CONCLUSION

By summing infinitesimal Lorentz transformations, we arrived at the metric tensor for an accelerated observer, which led to the equation of motion of a free particle for the accelerated observer. The equation reduces to the correct Newtonian result in the appropriate limit. Moreover, it provides an independent way to arrive at the *Thomas precession* effect.

ACKNOWLEDGMENT

This work is part of a more general project, “Relativistic generalization of inertial forces”, that includes both translational acceleration as well as rotation. The project was done at Center For Basic Sciences (CBS), Mumbai, as part of regular curriculum. I thank CBS for giving me the opportunity to do the project. I also thank Prof. Arvind Kumar for his guidance during the project without which this work would not have been possible.

References

[1] Hrvoje Nikolić, in *Relativity in rotating frames*, Eds. G. Rizzi and Ruggiero, Chapter 14, (2004) 275.
[2] R. A. Nelson, J. Math. Phys. 28, (1987) 2379.
[3] J. D. Jackson, *Classical electrodynamics*, 3rd ed. (Wiley India, 2007).
[4] J. V. Narlikar, *An introduction to relativity* (Cambridge University Press, 2010).
[5] Mritunjay Kumar Verma, *Relativistic generalization of inertial forces*, Project Report, Center for Basic Sciences, Mumbai, 2011 (Unpublished).

PROBLEMS IN PHYSICS

Readers are invited to submit the solutions of the problems in this section within two months. Correct solutions, along with the names of the senders, will be published in the alternate issues. Solutions should be sent to: H.S. Mani, c/o A.M. Srivastava, Institute of Physics, Bhubaneswar, 751005; e-mail: ajit@iopb.res.in

Communicated by H.S. Mani

1. Consider an electric dipole made of two particles each of mass m and charges Q and $-Q$ connected by a massless rod of length $2a$ with the centre of the rod fixed at the origin and the rod is free to rotate about the centre.

   There is a uniform magnetic field $\vec{B} = B\hat{k}$ along the $z-$axis.

   (a) Using spherical polar co-ordinates $(r = a, \theta, \phi)$, obtain the equations of motion for the charged particles.

   (b) Obtain the constants of motion.

   (c) Discuss small oscillations about $\theta = 0$.

2. Consider the Pauli spinor

   $$\psi = \begin{pmatrix} \alpha \\ \beta \end{pmatrix}.$$

   Show that there is direction $\hat{n}$ such that

   $$\vec{\sigma}.\hat{n}\,\psi = \psi$$

   Find $\hat{n}$ in terms of α and β. ($\vec{\sigma}$'s are Pauli spin matrices.)

   However this is not true for spins grater than $\hbar/2$. Thus for a spin 1 system there are states ϕ, represented by a column matrix of the form

   $$\phi = \begin{pmatrix} \alpha \\ \beta \\ \gamma \end{pmatrix} \quad (1)$$

   which are not eigenstates of $\vec{S}.\hat{n}$ with eigenvalue $\hbar$. ($\vec{S}$ are 3×3 matrices - the components of $\vec{S}$, S_1 , S_2, and S_3 satisfy the usual angular momentum commutation relations) Construct an example of such a vector.

Solutions to the problems given in Vol. 4 No. 4 of Prayas

Solutions provided by: H.S. Mani

Problem 1: The vector potential is defined by the equation $\vec{B} = \vec{\bigtriangledown} \times \vec{A}$ and by applying Stokes theorem we see that the loop integral $\int_c \vec{A}.\vec{dl}$ = $\int \vec{B}.\vec{dS}$ where the surface integral is over an area with its boundary as the loop c (with the contour c being in the counter clock-wise direction). This is the magnetic flux enclosed by the closed loop c. This is true irrespective of the size of the loop.

Consider now the case of a thin current carrying solenoid situated on earth, with flux ϕ through it. The loop c surrounding the solenoid is taken to be circular, concentric with solenoid, and has radius R. Take R to be extremely large, say distance to the moon. The above expression tells us that as soon as the flux ϕ is changed on the earth, $\vec{A}$ on the loop (at distance R away from the solenoid) must change instantaneously. How is this consistent with Special Relativity ?

Solution to Problem 1:

If the loop is very far away the flux enclosed by it zero as the most of the magnetic lines which come out of the solenoid return back and changes of the flux is felt only near the vicinity of the solenoid. For the flux to change in the loop the size of the solenoid should be of the order of the loop.

Saying it differently, far away from the loop the contribution of any localised current distribution is given by dipole which falls as $\frac{1}{r^3}$ and hence the vector potential falls of as $\frac{1}{r^2}$, where r is distance of the point of observation from the current distribution. Thus $\oint \vec{A}.\vec{dl}$ does not get any contribution. Only the "radiating terms" from the time dependent current distribution has $\frac{1}{r}$ behaviour but this is retarded and reaches the loop after a time interval determined by the speed of light.

Problem 2: Consider two one-dimensional coupled simple harmonic oscillators described by the Hamiltonian

$$H = \frac{p_1^2}{2m_1} + \frac{p_2^2}{2m_2} + \frac{1}{2}(k_1\, x_1^2 + k_2\, x_2^2 + k_{12}\, x_1\, x_2)$$

Find the energy levels of the system.(here p_1, p_2, x_1, x_2) refer to the momenta and coordinates of the two harmonic oscillators respectively. m_1, m_2 are their respective masses.)

Solution to Problem 2:

Let

$$x_1' = (\frac{m_1}{m_2})^{-(\frac{1}{4})} x_1;\ p_1' = (\frac{m_1}{m_2})^{(\frac{1}{4})} p_1$$

and

$$x_2' = (\frac{m_1}{m_2})^{(\frac{1}{4})} x_2;\ \ p_2' = (\frac{m_1}{m_2})^{-(\frac{1}{4})} p_1$$

This ensures $[x'_i, p'_j] = i\hbar\, \delta_{ij}$ with $i, j = 1, 2$ and the Hamiltonian becomes

$$H = \frac{p_1'^2}{2\sqrt{m_1 m_2}} + \frac{p_2'^2}{2\sqrt{m_1 m_2}} + \frac{1}{2}[k'_1 x_1'^2 + k'_2 x_2'^2 + k'_{12}\, x'_1 x'_2]$$

where

$$k'_1 = (\frac{m_1}{m_2})^{-\frac{1}{2}} k_1;\ k'_1 = (\frac{m_1}{m_2})^{\frac{1}{2}} k_2;\ k'_{12} = k_{12}$$

The potential energy term can be written as

$$\begin{pmatrix} x'_1 & x'_2 \end{pmatrix} \begin{pmatrix} k'_1 & \frac{k'_{12}}{2} \\ \frac{k'_{12}}{2} & k'_2 \end{pmatrix} \begin{pmatrix} x'_1 \\ x'_2 \end{pmatrix}$$

The eigenvalues of the 2×2 matrix are

$$K_\pm = \frac{(k'_1 + k'_2) \pm \sqrt{(k'_1 - k'_2)^2 + k_{12}'^2}}{2}$$

Since the diagonalization can be achieved by a unitary transformation,

$$\begin{pmatrix} X_1 \\ X_2 \end{pmatrix} = (U) \begin{pmatrix} x'_1 \\ x'_2 \end{pmatrix}$$

$$\begin{pmatrix} P_1 \\ P_2 \end{pmatrix} = (U) \begin{pmatrix} p'_1 \\ p'_2 \end{pmatrix}$$

The hamiltonian becomes

$$H = \frac{P_1^2 + P_2^2}{2m} + \frac{1}{2}[K_+ X_1^2 + K_- X_2^2]$$

where $m = \sqrt{m_1 m_2}$. We continue to have $[X_i, P_j] = i\hbar\delta ij,\, i, j = 1, 2$

The energy levels are

$$E = \hbar(\Omega_+ n_+ + \Omega_- n_- + 1)$$

where $\Omega_\pm = \sqrt{\frac{K_\pm}{m}}$ and $n_\pm$ take integer values $0, 1, \ldots$...

....

STUDENT JOURNAL OF PHYSICS

IAPT

Volume 4 **Number 6** **Jan.-Mar. 2013**

Contents

Published on behalf of Indian Association of Physics Teachers, 128/2, J.P. Naik Road, Kothurd, Pune-411 038, Phone : 020 25455504

Printed by Centre for Academic and Social Advancements, B/86, Krishna Garden (PH-II), Jagamara, Bhubaneswar - 751030